Nature Environment and Pollution Technology
An International Quarterly Scientific Journal

p-ISSN: 0972-6268
(Print copies up to 2016)
e-ISSN: 2395-3454

Vol. 22 | No. 1 | pp. 15-28 | 2023

Original Research Paper

https://doi.org/10.46488/NEPT.2023.v22i01.002

Open Access Journal

Pattern Characterization of Meteorological Drought Using Multivariate Drought Index Over Mirzapur in Middle Gangetic Plains of India

Shivani Gond*†, Nitesh Gupta, P. K. S. Dikshit* and Shyam Bihari Dwivedi***

*Department of Civil Engineering, Indian Institute of Technology (BHU), Varanasi, 221005, Uttar Pradesh, India

**Department of Civil Engineering, Sagar Institute of Research & Technology (SIRT), Bhopal, 462041, Madhya Pradesh, India

†Corresponding author: Shivani Gond; shivanigond@gmail.com

Nat. Env. & Poll. Tech.
Website: www.neptjournal.com

Received: 19-06-2022
Revised: 05-08-2022
Accepted: 10-08-2022

Key Words:
Multivariate drought index
Wet event
SPEI
Run theory
Pattern characterization
Variable-sized cluster analysis

ABSTRACT

Droughts and floods have been occurring at a higher frequency in recent decades. The rapid transition between them magnifies the socio-economic consequences of these catastrophes relative to the effects of the individual occurrences of the extreme event. This study examines the temporal variability of meteorological drought and wet event characteristics occurring over Mirzapur (Uttar Pradesh), India. The Standardized Precipitation Evapotranspiration Index (SPEI) is applied to monthly water balance at scales 3, 6, 9, and 12 months to estimate the meteorological drought and wet events from 1971 to 2018. Drought and wet event characteristics such as the number of drought/wet events, severity, duration, and intensity are estimated using run theory over SPEI output. While characterizing the pattern of trends over the historical time period, variable-sized cluster analysis (VSCA) allows the detection of multiple change points as opposed to the Mann-Kendall (MK) test, which produces a monotonic trend for the entire time period. The VSCA technique accounts for drought variability and depicts the pattern's evolution across the period under consideration. Station-scale drought data from Mirzapur, Uttar Pradesh (UP), India, were used in the procedure. VSCA allows for the detection of many change points while describing the pattern of drought trend throughout a historical period, as opposed to the usual Mann-Kendall (MK) test, which provides a monotonic trend for the whole time. As a result, VSCA demonstrated the MK test compatibility.

INTRODUCTION

There is growing evidence of increasing events of hydrologic extremes (drought and flood) becoming more regular due to the impact of recent warming, which significantly alters the global hydrologic cycle. The climate system comprises interdependent and dynamic mechanisms that fluctuate randomly within a fixed range of variability. The climate system consists of interdependent and dynamic mechanisms that fluctuate randomly within a static envelope of variability (Gupta et al. 2022). On the other hand, the precipitation and temperature characteristics alter with the anthropogenic changes in the earth (Omar et al. 2019a, 2020, Srinivas & Saral 2007). Heatwaves and humid heat stress in South Asia are expected to become more common and severe in the coming decades, according to the IPCC's Sixth Assessment Report (AR6). Increased yearly and summer monsoon precipitation variability means higher totals (Bhagawati et al. 2017, Varughese 2017). In most situations, water resources are examined separately for features related to wet and dry occurrences. Hydrologic and atmospheric dynamics are intertwined in a way that might exacerbate hydro-climatic variability under the impact of climate change (Omar et al. 2020, He et al. 2017). Drought is one of the hydrologic extremes that causes the most harm because it is so complicated and recurrent. Decreased precipitation for an extended period in a vast geographic region causes considerable damage to the environment and human livelihoods across the world (Subbiah et al. 2021). This increase in temperature exacerbates the severity of drought. Therefore, It is necessary to utilize a wide range of drought indicators to monitor a wide range of hydrologic cycles and processes due to a variety of different types of meteorological, agricultural, and hydrological droughts that have been seen in recent decades (Nabaei et al. 2019, Qutbudin et al. 2019, Rosalia & Hakim, 2021, Tan et al. 2015, Mishra & Singh 2010). SPI and SPEI are widely acknowledged for practical drought monitoring among the many drought indicators, as are the limits of each. The input parameters for SPI and SPEI are different, but the mathematical computations are equivalent. Climate

inputs used by SPI models include simply precipitation, whereas those of SPEI models also have information on climate water balance. Many studies recommend employing SPEI rather than SPI because of its relation to potential evapotranspiration (PET), which is more sensitive to global warming (Vicente-Serrano et al. 2010, Huang et al. 2017). Studying historical drought occurrences may be aided by understanding regional patterns in terms of drought severity, length, and geographical extent. Drought episodes and their effects can also be predicted more accurately (Mallya et al. 2015). Due to the varied geological and climatic conditions on the Indian subcontinent, Indian agriculture is too complex for irrigated and dry land areas (Omar et al. 2019b).

Various studies have evaluated the trend of drought variability over the considered period using the nonparametric Mann-Kendall (M.K.) test (Bacanli 2017, Dashtpagerdi et al. 2015). Guhathakurta et al. (2017) analyzed the trend variability of monthly SPI for the monsoon season using the M.K. test at a 95% significance level. They noted a significant rise in the drought occurrence over the districts of India (Pandey et al. 2021). Over the post-monsoon season, a substantial rise in drought severity and the event was found by conducting the M.K. test on SPI output in the Bundelkhand area. However, the monotonic trend of climatic parameter time series generally does not display monotonic behavior but rather nonperiodic alternating behavior at an intermediate period when using the Mann-Kendall (M.K.) approach. Typical parametric and nonparametric tests may miss real-time information that varies from the aggregation in aggregated data sets. Non-stationarity in hydrological systems leads to shifts in average precipitation, frequency of severe events, evapotranspiration amplitude, and river flow. The complex interconnectedness and dynamic dynamics of climatic variables continually update hydrometeorological processes and contribute to the non-stationarity of climatic variables. Gupta et al. (2021) introduce the methodology to assess the change in the trend pattern, which incorporates the intermediate variation of the climatic variable over the study period. Singh et al. (2019) advised that drought-resistant crops should be grown in Mirzapur (Uttar Pradesh) throughout the Ravi season, according to a study that examines the probability of dry and wet periods and the likelihood of successive dry and wet spells. The development of understandable maps of spatial rainfall patterns that depict temporal variations and highlight hazards related to water scarcity and drought, as well as the vulnerability assessment of ecosystems, agriculture, water resources, and socioeconomic contexts to drought risk, need to be the main focus of future research.

There must be early knowledge of the length and scope of the water scarcity if precautions against moisture stress in crops are to be taken. Using weather data from the past 30 years (1984-2013), scientists have come up with a way to predict how much water crops need each week in Mirzapur, District (Uttar Pradesh) in the Vindhya Zone of the Indo-Gangetic Plains (Singh et al. 2019). Gond et al. (2019) examined SPI and SPEI at multiscale for their temporal variability in the severity of drought, and their trend assessment by applying M.K. tests conducted in Mirzapur District revealed that SPEI accounts for a higher number of events with a higher magnitude of the district's droughts than SPI. The Theory of Runs is a time series analysis method that has been frequently employed in drought event identification (Zhang et al. 2015). Its fundamental challenge is determining the intercept level. Many earlier studies merely set a single intercept level in the Theory of Runs (Liu et al. 2016). This method was straightforward, but it tended to overidentify or under-identify drought characteristics, lowering the accuracy of the data. As a result, further optimizing the interception level of drought detection and testing more distinct drought index thresholds are required so that the drought events identified are consistent with the actual ones. There was a lack of attention paid to the wet event features in all the investigations in the aforesaid context.

Consequently, in this work, we aimed to examine the drought and wet parts of Mirzapur (Uttar Pradesh), India. The location's monthly means temperature and longitude are input variables in Thornthwaite's method to calculate potential evapotranspiration (PET) (Thornthwaite 1948). SPEI was used to estimate drought and wet occurrences over a period of three, six, nine, and twelve months from 1971 to 2018. The severity, duration, and intensity of dry and wet event characteristics were calculated by applying the run theory to the SPEI output. The VSCA technique was utilized to account for drought variability and depict the evolution of the pattern during the time period under consideration.

Study Area and Data Used

The district of Mirzapur in Uttar Pradesh (India), located on the Vindhyan Plateau in the middle Gangetic plain and covering a total area of 4,521 km^2, is being studied for this present objective. Mirzapur stretches between 23°52′ to 25°32′ North latitude and 82°07′ to 83°33′ East longitude (Fig. 1). The Mirzapur district has two immediate reliefs, the Alluvial Ganga plains in the north and the Vindhyan Plateau in the south. Soil is available in various forms, from alluvial to sandy to red. Red and black soils predominate in plateau regions (Census of India 2011). The humid subtropical climate (Köppen classification Cwa) characterizes the weather in Mirzapur, which has dry winters. The average annual rainfall occurs at 997.40 mm a year, with 75 to

80 percent of the rainfall coming from the Bay of Bengal monsoonal system during the monsoon season (June to September). And the temperature extremes were observed during summer (42 to 45°C) and winter (8 to 10°C). The average relative humidity is 42.2 %, ranging from 42.2 to 70.5 %. In rainfed sections of the district, farmers plant paddy as a primary crop during the Kharif season (90 % of total farmed land) and mustard, lentil, chickpea, and pea during the rabi season on residual moisture.

SPEI index is adopted to evaluate the temporal pattern of meteorological drought and wet events over the research area. It requires monthly precipitation (P) and potential evapotranspiration (PET) as input climate variables to estimate drought and wet events at the timescale of 3 months, 6 months, 9 months, and 12 months. The Thornthwaite method was used to calculate potential evapotranspiration. From 1971 to 2018, the monthly weather data (rainfall and temperature) were obtained from the Indian Meteorological Department (IMD) and the Indian Water Portal (https://www.indiawaterportal.org/met_data).

MATERIALS AND METHODS

Potential Evapotranspiration (PET)

Potential evapotranspiration (PET) is the potential of the atmosphere to remove the maximum amount of water by evaporation and transpiration from the uniformly vegetated surface without any limitation's other atmospheric demands. The critical factors limiting the rate of potential evapotranspiration are the sun's radiative energy, wind, the vapors deficit of the air, and temperature. The Thornthwaite method, as given in equation 1, used to estimate PET requires only monthly average temperature as an input climatic variable (Thornthwaite 1948).

$$PET = 16d\left(\frac{10T}{I}\right)^{a} \quad \ldots(1)$$

Where d is the correction factor, T (°C) means monthly temperature, I denote the annual thermal index, and i is the monthly thermal index. These variables can be calculated as follows:

$$I = \sum_{j=i}^{12} i \quad \ldots(2)$$

$$i = \left(\frac{t}{5}\right)^{1.514} \quad \ldots(3)$$

$$a = 0.49 + 0.018I - 7.7x10^{-5} I^2 + 6.7x10^{-7} I^3 \quad \ldots(4)$$

Standardized Precipitation Evapotranspiration Index (SPEI)

The standardized evapotranspiration index (SPEI) is a multivariate drought index established by Vicente-Serrano et al. (2010), which considers the impact of temperature

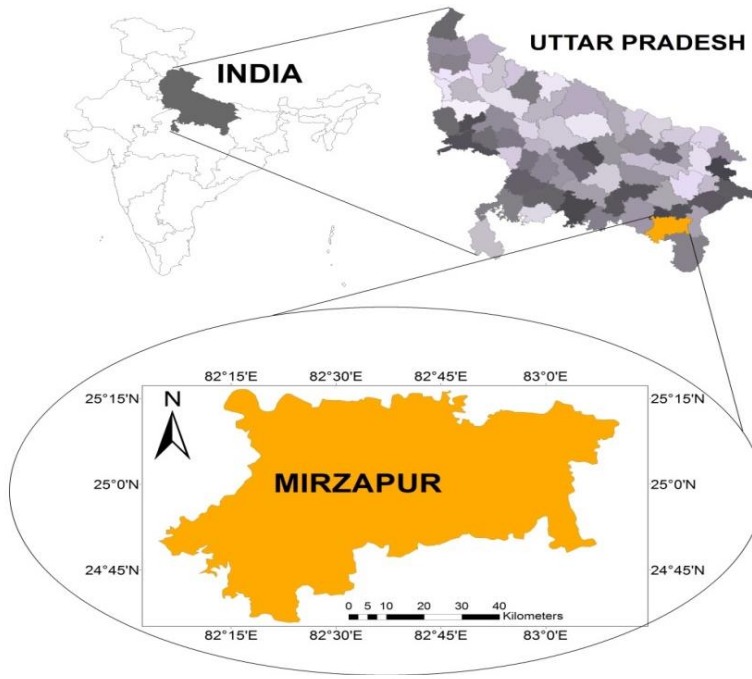

Fig. 1: Geographical map of the Mirzapur district of Uttar Pradesh, India.

Table 1: Categorization of the severity of drought and wet events based on SPEI values.

SPEI	Severity	SPEI	Severity
Extreme drought	<-2	Moderately Wet	1.49 to 1.0
Severe drought	-1.5 to 1.99	Very Wet	1.99 to 1.5
Moderate drought	-1.0 to -1.49	Extremely Wet	2≤
Near Normal	0.99 to -0.99	-	-

variation on drought severity (Liu et al. 2021). Climate factors such as precipitation and temperature, which influence water availability and variability, are considered in the classification of drought severity. SPEI takes water balance (P-PET) as input climatic at different accumulation periods. The non-exceedance probability of water balance ($Di = P_i - PET_i$) (equation) determines the SPEI values. The method for calculating the SPEI value is described in detail (Pei et al. 2020, Polong et al. 2019, Tan et al. 2015).

The calculated D values are accumulated at different time scales

$$D_n^k = \sum_{i=0}^{k-1} P_{n-1} - (PET)_{n-1} \quad \ldots(5)$$

K is the timescale (months) of accumulation, and n is the calculation month.

The probability density function of a Log-logistic distribution is given as follows:

$$f(x) = \frac{\beta}{\gamma}\left(\frac{x-\gamma}{\alpha}\right)^{\beta-1}\left(1+\left(\frac{x-\gamma}{\alpha}\right)^{\beta}\right)^{-2} \quad \ldots(6)$$

where α, β, and γ are scale, shape, and origin parameters, respectively, for $\gamma > D < \infty$. The probability distribution function for the D series is given as follows:

$$F(x) = \left[1+\left(\frac{\alpha}{x}-y\right)^{\beta}\right]^{-1} \quad \ldots(7)$$

With f(x) the SPEI can be obtained as the standardized values of F(x):

Where, $SPEI = W - \frac{C_0+C_1W+C_2W^2}{1+d_1W+d_2W^2+d_3W^3}$ …(8)

$$W = \sqrt{-2\ln(P)} \text{ for } P \leq 0.5 \quad \ldots(9)$$

P is the probability of exceeding a determined D_i value and is given as

$P = 1 - f(x)$ while the constants are:

$C_0 = 2.515517$, $C_1 = 0.802853$, $C_2 = 0.010328$, $d_1 = 1.432788$, $d_2 = 0.189269$, $d_3 = 0.001308$

Characteristics of Drought and Wet Events

Drought and wet episode characteristics are defined by severity, intensity, and duration, determined by the run theory given by Yevjevich (1969). A run is a period in which all the index values fall below a predetermined threshold (Yevjevich 1969). Researchers in the literature have used various thresholds to estimate drought parameters (Mesbahzadeh et al. 2020, Pandey et al. 2021). Based on SPEI output, drought and wet event parameters were estimated at the threshold of SPEI <-1 to evaluate drought/ wet event characteristics. When SPEI values are consistently negative and reach a value of -1 or below, it is considered a drought event, and when SPEI value comes to 1 or above, it is considered a wet event (Table 1).

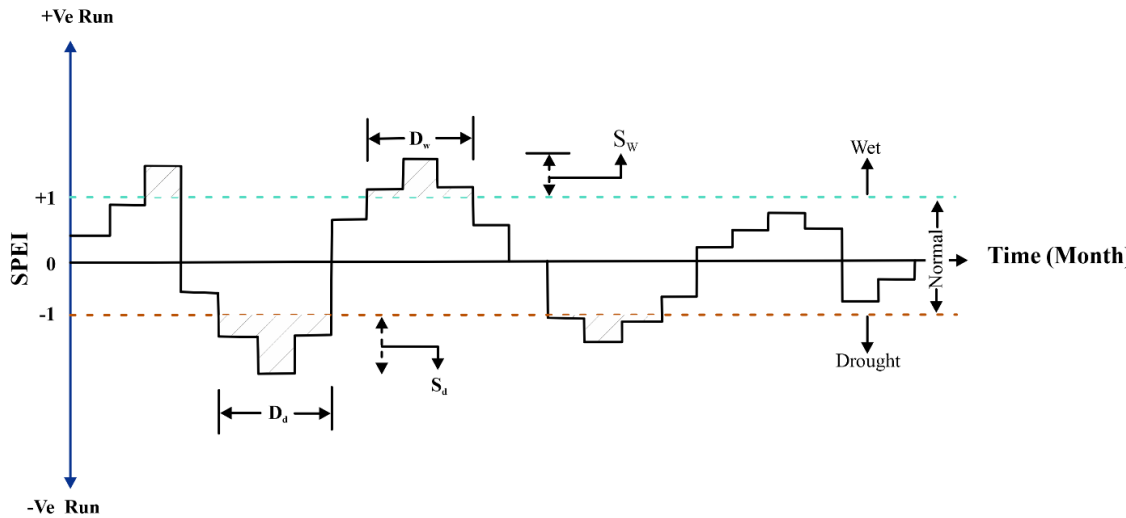

Fig. 2: Run theory-based drought and wet characterization (Malik et al. 2021).

Drought and Wet Severity (S_d and S_w)

During droughts and wet events, severity is calculated as the absolute value of indices.

$$S_d = |\sum_{n=1}^{D} \text{SPEI}| \leq -1 \quad \ldots(10)$$

$$S_w = |\sum_{n=1}^{D} \text{SPEI}| \geq 1 \quad \ldots(11)$$

Drought and Wet Duration (D_d and D_w)

It is defined as months between the start and end of a drought event when SPI/SPEI ≤ -1 and during wet during the event when SPEI ≥ 1.

Drought and Wet Intensity (I_d and I_w)

During a drought and wet event, the ratio of the absolute value of drought and wet severity to the duration of the drought and the wet event is computed as drought and wet intensity (I_d and W_d).

$$I_d = \frac{S_d}{D_d} \quad \ldots(12)$$

$$I_w = \frac{S_w}{D_w} \quad \ldots(13)$$

Variable-Sized Cluster Analysis

For trend analysis, rather than the traditional approach of using Pettitt Mann Whitney's method, which yields a single long-term trend, the provided form uses variable-size cluster analysis, which provides a visual representation of the changing trend pattern as well as hints to identify one or several change points and/or alternate trends (Gupta et al. 2021). Drought trend variation was clearly illustrated by 3-D figures created for Z-score variability with varied starting and ending periods. This was not apparent by a conventional M.K. test, including the whole historical dataset. Trend analysis based on station scale data was more accurate than grid-based data based on spatial averaging. A more accurate result may be drawn when numerous clusters were created by successively deleting data from the beginning of each year in the M.K. test.

It was necessary to apply the Mann-Kendall test many times to provide a reliable picture of the effect of drought in the Mirzapur area of Uttar Pradesh. Although it was first set to 5, 10, 15, and 20 to check if the results of the research were influenced, it was ultimately set at 10 for the repeated application of the Mann-Kendall trend test for all districts. The following equation was used to determine how many times the Mann-Kendall test would have to be run in a given district:

$$N = \frac{[(n-8).(n-9)]}{2} \quad \ldots(14)$$

The two-and three-dimensional planes were used to depict the Z values obtained from each MK test application. Z values are shown in 3-D for the first time in this study. Each of the graphs in this section shows the time at which each data cluster is picked for Z-value determination, as shown in Fig. 5(a)-8(a). Alternatively, the Z-statistic may be seen in various colors in the upper left triangle region of Images 5(b)-8(b) from the top viewpoint of Images 5(a)-8(a). As one goes across the graphical plane, the size of the data cluster is utilized to compute the Z-statistic changes. This is seen in Figs. 5(a)-8(a), where the Z statistic values correspond to variable-sized data clusters with varying starting and ending durations (a). These variable-sized data clusters may assess drought trend patterns using different Z-statistic values. The magnitude of the Z-statistic was depicted using a Z-axis normal to the X-Y plane; as a result, these images provide a 3-D graphical viewpoint of an erratic surface spread according to various Z-statistic values.

Z values are shown in 3-D in this work, which is a novel feature. The numbers indicate data clusters selected for Z value determination on the abscissa and ordinate axes in Figs. 5(a)-8(a). As Figs. 5(b)-8(b), the Z-statistic can be shown in various shades of color in the top left triangle of the figures. On the graphical plane, the size of the data cluster is utilized to compute the Z-statistic changes as illustrated in Fig. 5(a)-8(a), which shows the Z statistic values for variable-sized data clusters with varied beginning and ending durations. It is possible to calculate multiple Z-statistic values, which may then be displayed to study the drought pattern and trend. Using a Z-axis (Z-axis) normal to the X-Y plane, these images display a 3-D viewpoint of an erratic surface spread in accordance with shifting Z-statistic values, as seen in these images.

Z-values with fixed window size (data cluster size) but growing start time are depicted in Figs. 5b-8b by a line parallel to the hypotenuse of the right-angled triangle. There are 10 data points in this window, and parallel lines on the hypotenuse represent the following window sizes 11, 12, 13, 14, and so on. Data from the first to the tenth, first to the eleventh, first to the twelfth, etc., are represented by dots on perpendicular vertical lines to the abscissa. Color variations in Fig. 5(a-b)-8(a-b) represent significant shifts in the drought trend, which are seen in the figures. Change points with multimodal characteristics cannot be detected using the Pettitt-Mann-Whitney test because it relies on a single maximum value of Ut for the entire time period, whereas variable-sized cluster analysis allows for the detection of multiple change points that may have occurred over the course of a century. When one or more changes occur throughout the research, VSCA can identify them.

RESULTS AND DISCUSSION

Meteorological Drought and Wet Characterization

A joint assessment of meteorological drought and wet period using SPEI at different accumulation periods of water balance

(P- PET) (3-month, 6-month,9- month, and 12-month) over Mirzapur (Uttar Pradesh) India for the period of years from 1971 to 2018. The negative value of SPEI indicates the drying condition from normal conditions, whereas the positive value of SPEI referred to as wet condition (Fig. 2). Meteorological drought characteristics, i.e., severity, intensity, and duration, and the number of drought occurrences estimated at the threshold of SPEI $\leq$ -1 similarly, wet event characteristics estimated at the threshold of SPEI $\geq$ 1. Fig. 4 indicate that a higher number of drought/ wet event of different categories recorded at a shorter time scale (SPEI-3, SPEI-6) indicate the seasonal variation of climatic water balance, which may cause an adverse impact on the crops of the study region. In contrast, at higher time scale (SPEI-9 and SPEI-12), the number of occurrence drought/wet event reduced but occurred with higher severity and persisted for a longer duration (Fig. 3 & Fig. 4), which indicate the SPEI's gradual and consistent response to changes in water balance annual scale. The study area dominantly experiences moderate drought-wet events during the study period. During the study period, a slightly higher number of meteorological drought events at every scale (SPEI-3=42, SPEI-6=30, SPEI-9=23, SPEI=20) were recorded in comparison with wet events (SPEI-3=40, SPEI-6=30, SPEI-9=24, SPEI12=11) Fig. 4 depicts the decadal shift in the occurrences of drought-wet events of various types, highlighting the most significant number of drought occurrences reported during the 2000s, followed by the 2000s. After 2000, the maximum number of wet occurrences was recorded throughout the 1970s and 1980s. As the decades progressed, the number of wet occurrences decreased, indicating drying up conditions over the study area.

The drought-wet event characteristics (severity, intensity, and duration) are summarized in Fig. 3 by combining a violine plot with a small box plot for different timescales for the study period, where the width of the violine denotes frequency, and the curve denotes the shape of the data. The thin black line represents the maximum and minimum value

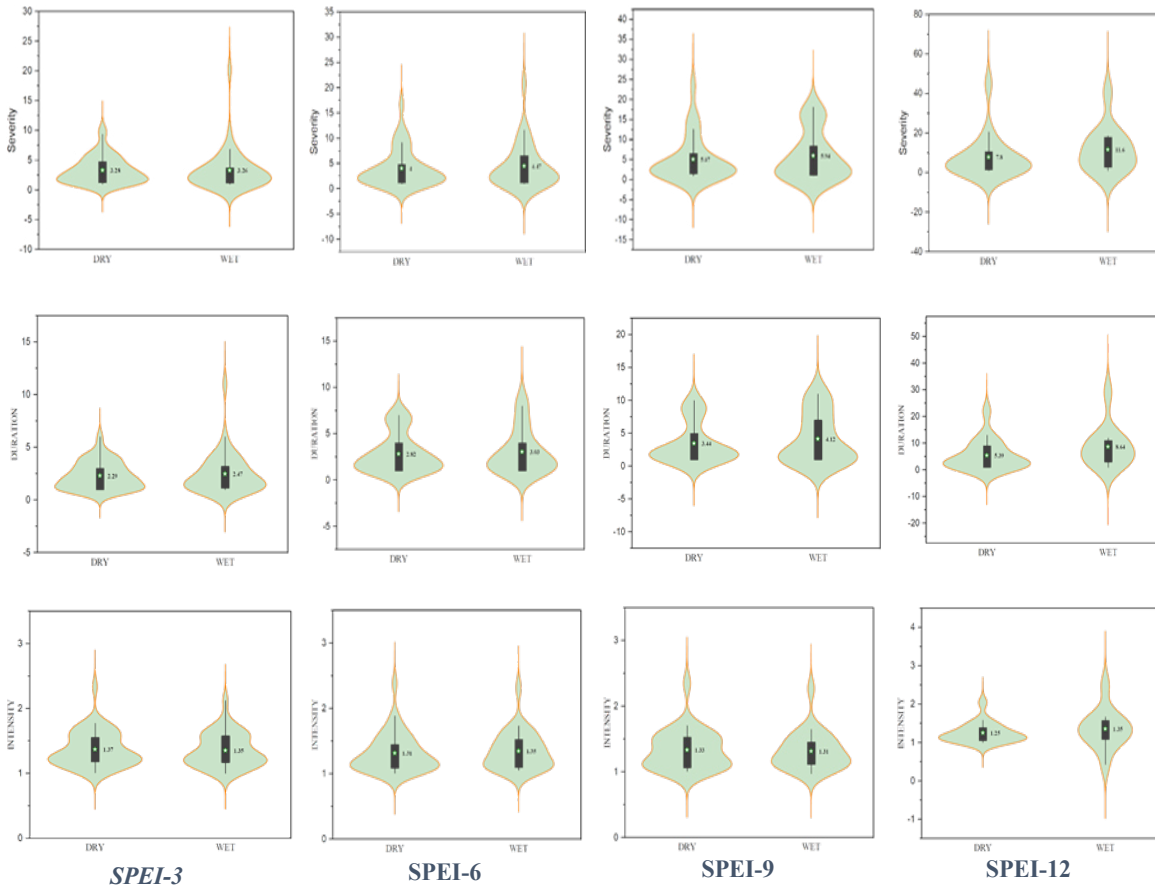

Fig. 3: Violine diagram with a small box plot explaining the drought and wet event characteristics (Severity, Duration, and Intensity) of SPEI-3, SPEI-6, SPEI-9, and SPEI-12 time series from 1971 to 2018. The density curve's width represents the data's frequency, and the small black box plot represents the first and third quartiles. The star sign in the center of the box plot represents the mean.

of drought-wet characteristics, and the star at the center of the box plot indicates the average of drought-wet characteristics. A greater of drought-wet events occurred as the timescale of SPEI progressed S_w (SPEI-3)=3.26, S_w (SPEI-6)=4.47, S_w (SPEI-9)=5.94, and S_w (SPEI-12)=11.6 which interestingly illustrates that wet event occurred with the severity of drought events S_d (SPEI-3)=3.5, S_d (SPEI-6)=5, S_d (Spei-9)=6.93, S_d (SPEI-12)=7.34. In contrast, the duration of the drought-wet event is D_d (SPEI-3)=2.4, D_d (SPEI-6)=3, D_d (SPEI-9)=4.12, D_d (SPEI-12) =2.2, D_w (SPEI-6)=2.8, D_w (SPEI-9)=3.4, and D_w (SPEI-12)=5.3, indicating that the drought episode persisted for a longer duration. As demonstrated in Fig. 3, the intensity of drought-wet episodes does not vary significantly with the timescale. Drought and wet events occurred at roughly the same intensity.

Pattern Characterization of Meteorological Drought

3-D and 2-D images of the drought trend over Mirzapur

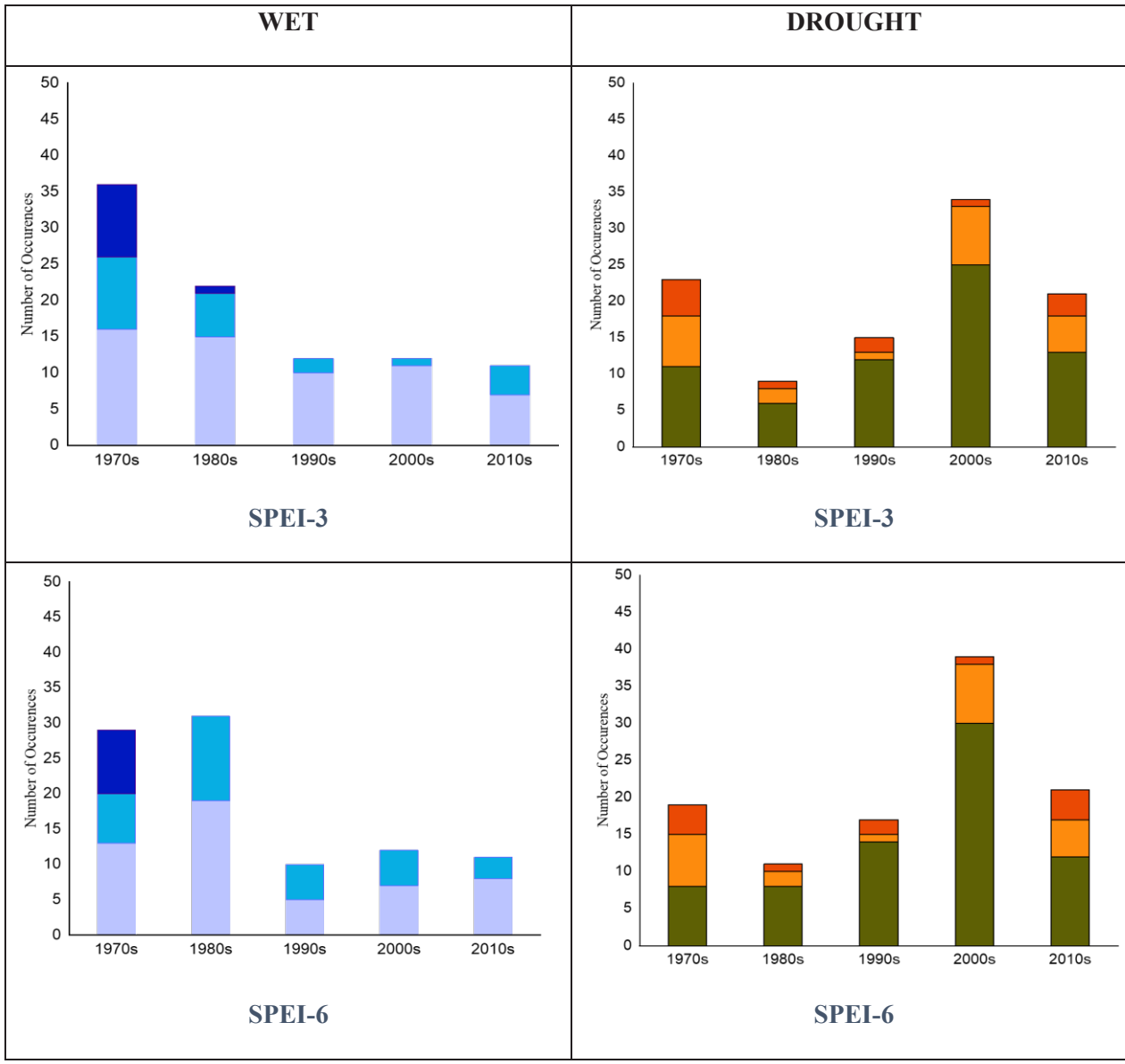

Fig. Cont....

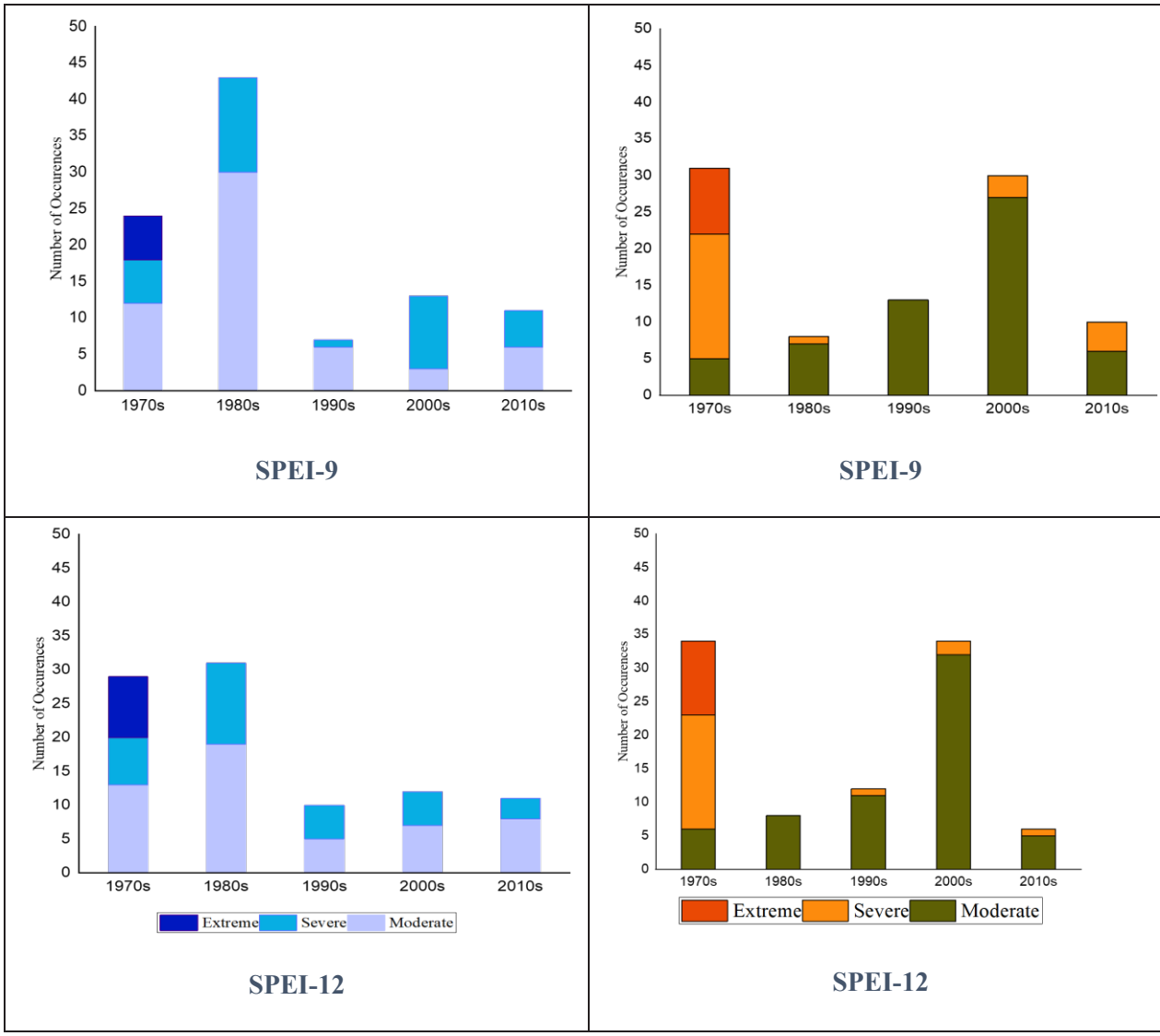

Fig. 4: Number of Drought and Wet events occurrences of different categories (Extreme, Severe, Moderate) of SPEI-3, SPEI-6, SPEI-9, and SPEI-12 during the last five decades, i.e., the 1970s, 1980s, 1990s, 2000s, and 2010s.

from 1971 to 2018 are shown in Figs. 5(a-b) and 8(a-b), respectively. There are many crests and troughs of different heights seen in Fig. 5a. The greater the height of the crests, the more intense and stronger the trend direction is. The trend's swings are reflected in the chart's many crests and troughs. Thus, the drought patterns in Mirzapur were shown to shift throughout time. There are basically three distinct zones in Fig. 5(a), each with a distinct set of troughs, crests, and low-amplitude troughs and high-amplitude crests (Zone-1, Zone-2, and Zone-3) (Zone-3). In Fig. 5(b), these zones are shown as patches of the same number. Zone-1 and patch-1 show a lessening tendency in drought conditions. Drought in Zone 2 and Patch 2 increased significantly during the 1960s compared to the previous decades. Zone-3, on the other hand, shows just a minor tendency for drought in either direction, with no notable characteristics.

The results of this cluster analysis with a range of cluster sizes can also be used to pinpoint the point(s) at which the drought pattern began to shift. As shown in Fig. 5(b), to draw a line separating Patches 1-2 from Patch 3, one must first project an imaginary straight line from Patches 1 and 2's maximum amplitude crest (see Fig. 5(a)) to Patch 3's least undulating surface (indicated along ending data 100). When these lines connect with the horizontal line, the tendency of drought undergoes a substantial shift over a number of years. Thus, the MK test-based VSCA anal-

ysis provided not only the drought trend but also a great capacity to pinpoint the time of change. The inflection line between zones 1 and 2 is the foundation for drawing the line separating patches 1 and 2 from each other. The difference in the drought trend might be considered a turning point in the differentiation of these zones. The increasing industrialization-induced urbanization is thought to be the cause.

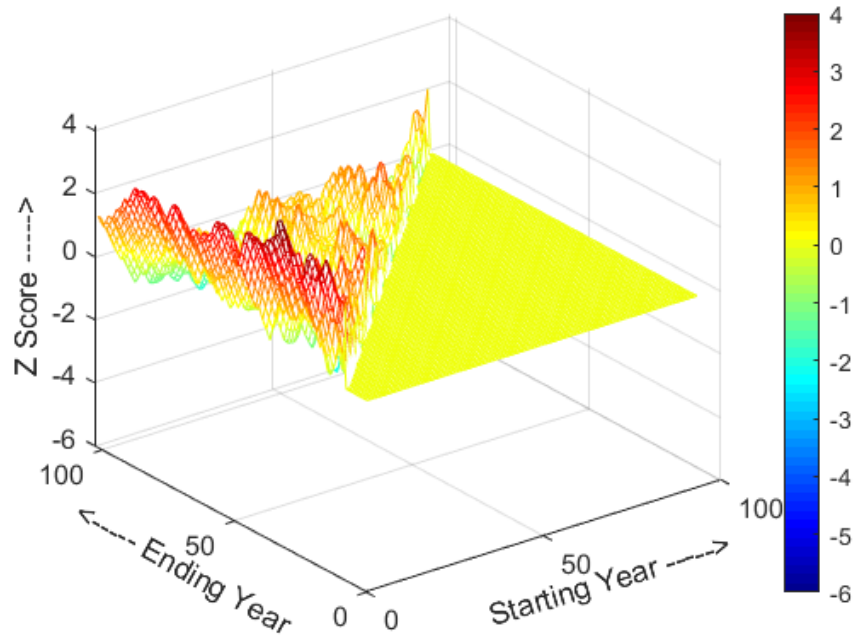

Fig. 5(a): 3-D characteristics of the pattern of drought trend at time scale 3 at significance level 0.05 for Mirzapur.

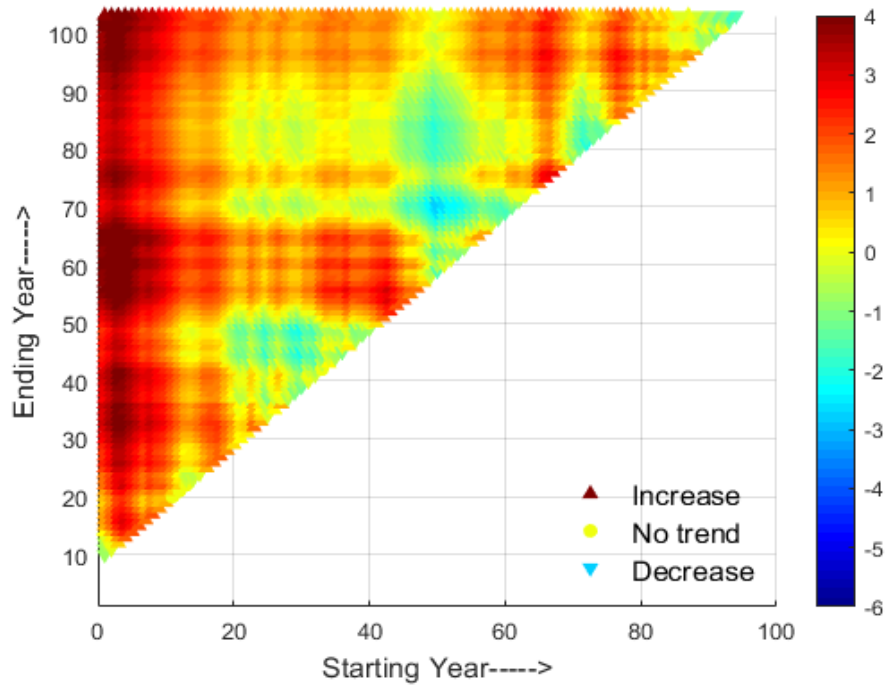

Fig. 5(b): 2-D characteristics of the pattern of drought trend at time scale 3 at significance level 0.05 for Mirzapur.

3D and 2D patterns of drought features for Mirzapur are shown in Figs. 6 (a-b). Several color shifts can be seen near the 100-point mark on the x-axis-parallel line that was drawn. The point at which something changes is called the change point. These spots around the 13th, 27th, 41st, and 73rd have disrupted drought patterns. Fig. 6(a) displays the trend's multimodal features, including two trough zones (equivalent to patches 1&3 in 2D Fig. 6(b)) and a crest zone (patch 2). The variable-sized cluster analysis may determine the various change points that may have happened in the provided historical drought data. As a result, if the research is lengthy enough, VSCA may be able to detect numerous

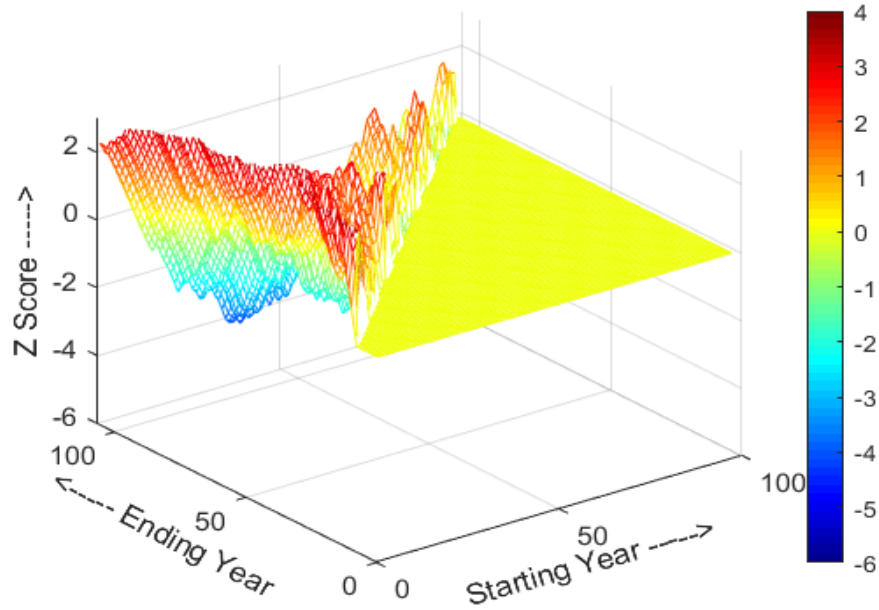

Fig. 6(a): 3-D characteristics of the pattern of drought trend at time scale 6 at a significance level of 0.05 for Mirzapur.

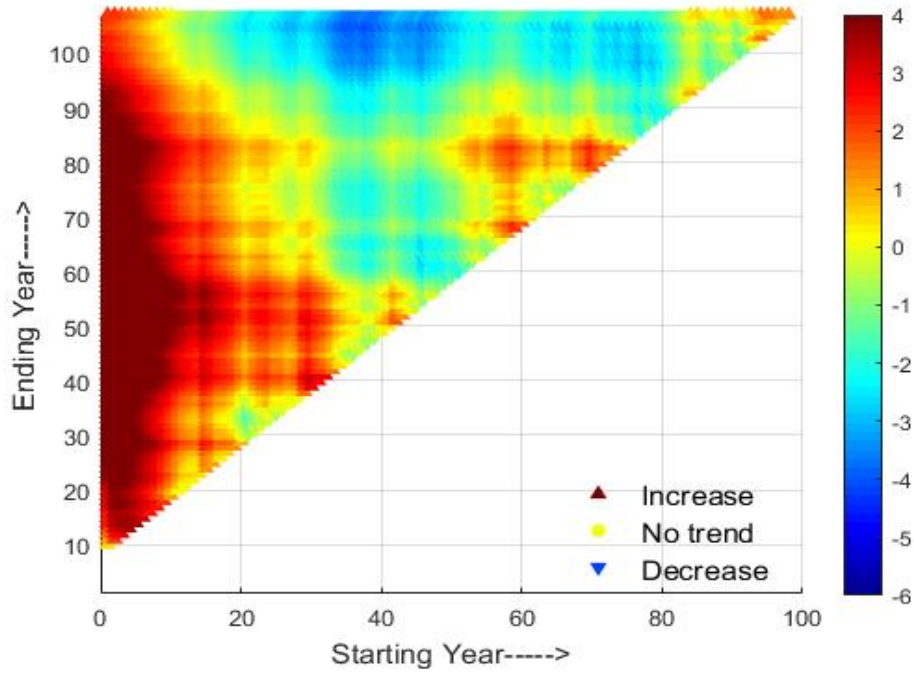

Fig. 6(b): 2-D characteristics of the pattern of drought trend at time scale 6 at significance level 0.05 for Mirzapur.

points of change. Fig. 6 and 7 show the same thing as in Fig.5(a) and (b).

Fig. 7 and 8 illustrate the 3D and 2D drought trends at time scale 9 for Mirzapur (a-b). As seen in 2D Fig 7(b), Fig 7(a) exhibits two troughs and one crest (patches 1 and 3). The multimodal trend pattern is clearly apparent in Fig 7(a). Comparing the data from the first decades of the drought series, a decrease in drought severity is seen in Zone 1

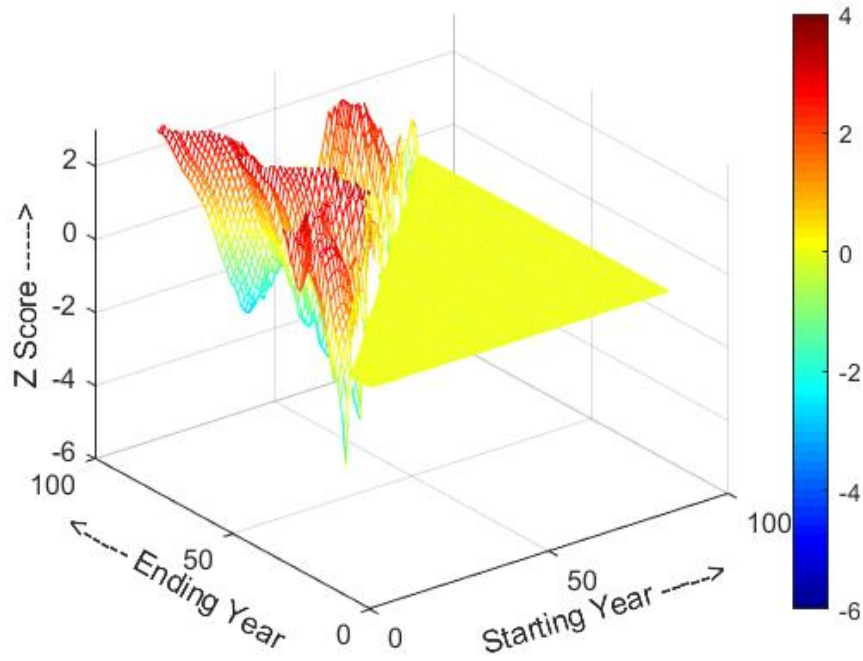

Fig. 7(a): 3-D characteristics of the pattern of drought trend at time scale 9 at a significance level of 0.05 for Mirzapur.

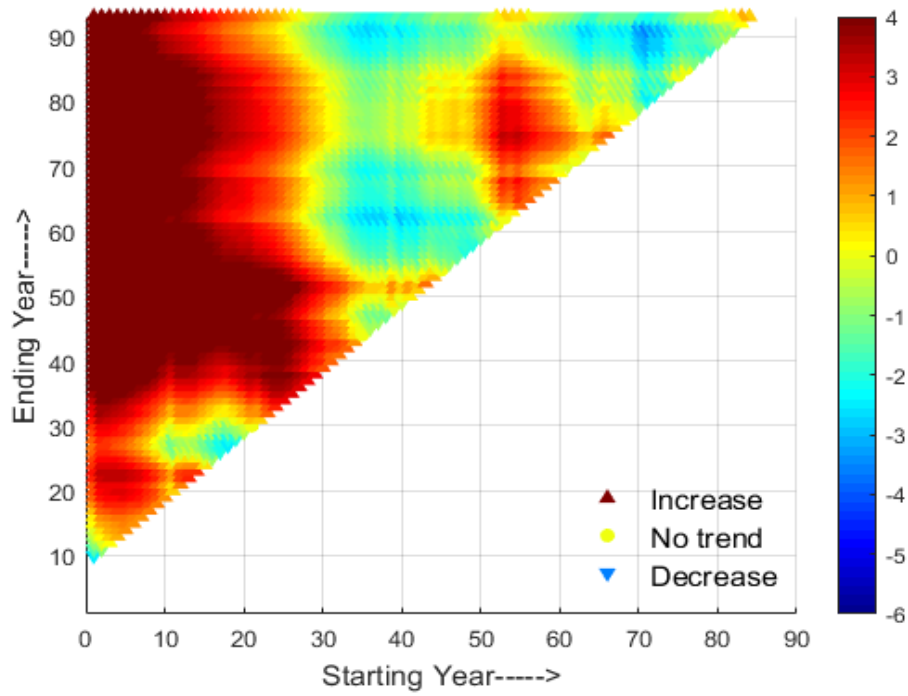

Fig. 7(b): 2-D characteristics of the pattern of drought trend at time scale 9 at a significance level of 0.05 for Mirzapur.

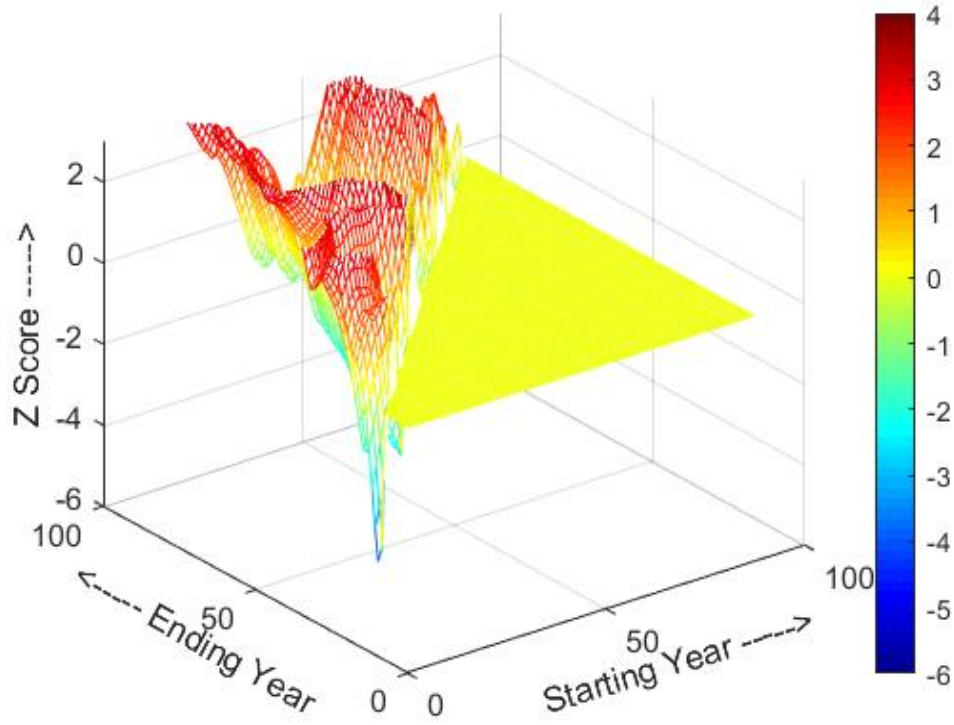

Fig. 8(a): 3-D characteristics of the pattern of drought trend at the time scale of 12 at a significance level of 0.05 for Mirzapur.

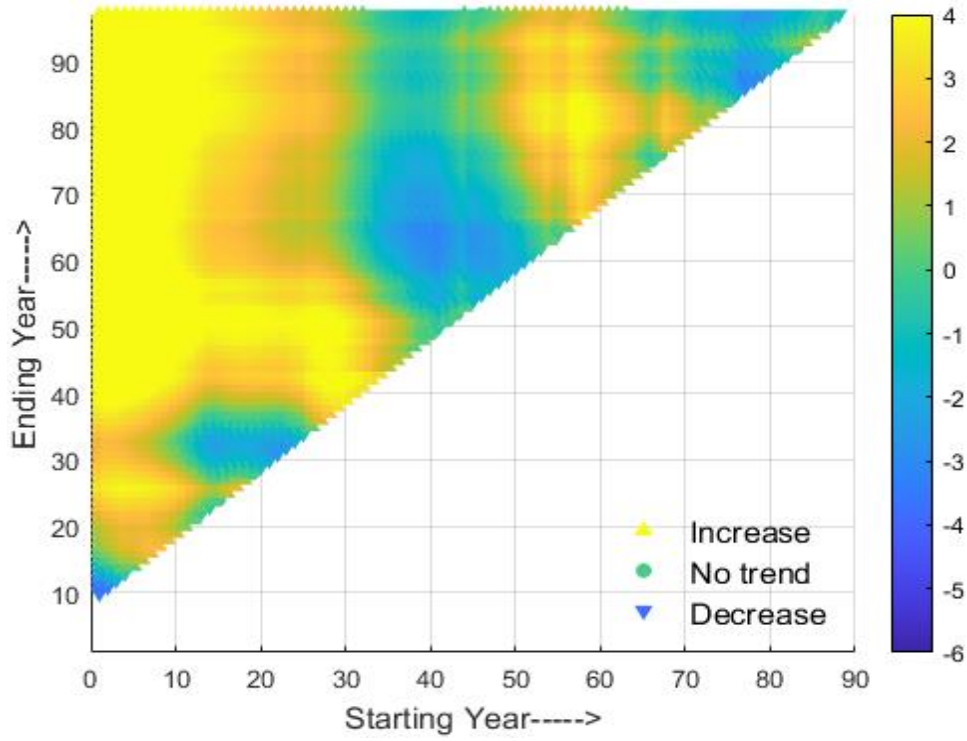

Fig. 8(b): 2-D characteristics of the pattern of drought trend at a time scale of 12 at a significance level of 0.05 for Mirzapur.

throughout the decades surrounding the 40th century. The line drawn parallel to the x-axis shows a significant break in the continuity of shades of hue. With regard to the total duration of the data series, this refers to a shift in the drought trend. In this case, the variable-sized cluster analysis could also show the trend pattern across multiple periods for a century's worth of data and identify the transition point. As a result, VSCA may be able to detect one or more change points if the research is long enough. Fig. 7 and 8 show the same thing as in Fig. 5(a) and (b).

For Mirzapur, 3D and 2D patterns of drought features are shown in Figs. 8(a-b). It is obvious that two patches 1-2, which split the two zones of crest and depression, may be seen in Fig. 8(a) and (b). Mirzapur's change sites were identified using the multimodal properties of the pattern of trend in Fig. 8(a) and the 2D pattern in Fig. 8(b). Ending time series data 100 is shown in the 2D Fig. 8 as an increase or decrease in color along a line drawn parallel to the x-axis (b). This is where a major shift in the trend has happened, according to the change in the continuity of colors. It's possible to see a change in trend around roughly data points 19 through 69 (On the x-axis). Fig. 8(a) clearly shows the crests and troughs that result from these many transition points. VSCA provided numerous change points to detect multiple change points.

CONCLUSION

The present study provides a joint assessment of drought-wet event characteristics and their temporal variability over the study period. The SPEI is used as proxies to estimate the meteorological drought–wet event, which incorporates the impact of global warming over the hydrologic extremes. The monthly SPEI was estimated at different accumulation periods (3-month, 6-month, 9-month, and 12-month) for the period 1971 to 2018. The assessment of temporal variability of drought–wet event occurrence indicates that the study area was primarily impacted by moderate category drought and wet conditions, followed by severe category drought and wet conditions, and extreme category drought and wet conditions, which occurred only infrequently over the course of the research. The decadal analysis of dry and wet event occurrences reveals a considerable increase in drought events after the 2000s, indicating a shift in climatic conditions over Mirzapur, which poses a threat to agriculture. To better understand the characteristics of drought and wet event severity, intensity, and duration, a threshold of one was used to determine that as the timescale grows, the severity and duration of an event increase, and the drought event occurs with greater severity and lasts longer. There is no discernible variation in the intensity of drought and wet events over timescales. The above analysis revealed that Mirzapur experiences a higher number of meteorological droughts with higher severity and longer duration.

REFERENCES

Bacanli, Ü.G. 2017. Trend analysis of precipitation and drought in the Aegean region, Turkey. Meteorol. Appl., 249: 239-249. https://doi.org/10.1002/met.1622

Bhagawati, R., Bhagawati, K., Jini, D., Alone, R.A., Singh, R., Chandra, A., Makdoh, B., Sen, A. and Shukla, K.K. 2017. Review on climate change and its impact on agriculture of Arunachal Pradesh in the Northeastern Himalayan region of India. Nat. Environ. Pollut. Technol., 6(2): 535-539.

Dashtpagerdi, M.M., Kousari, M.R., Vagharfard, H., Ghonchepour, D., Hosseini, M.E. and Ahani, H. 2015. An investigation of drought magnitude trend during 1975–2005 in arid and semi-arid regions of Iran. Environ. Earth Sci., 73(3): 1231-1244. https://doi.org/10.1007/s12665-014-3477-1

Gond, S., Gupta, N. and Gupta, S. 2019. Evaluation of Drought Severity Indices and their Trend for Mirzapur (Uttar Pradesh). December 2019. 24th International Conference on Hydraulics, Water Resources and Coastal Engineering (HYDRO 2019 International), 18-20 December 2019, Hyderabad, India, Osmania University & The Indian Society for Hydraulics, Hyderabad & Pune, pp. 2275-2283

Guhathakurta, P., Menon, P., Inkane, P.M., Krishnan, U. and Sable, S.T. 2017. Trends and variability of meteorological drought over the districts of India using standardized precipitation index. J. Earth Syst. Sci., 126(8): 1-18. https://doi.org/10.1007/s12040-017-0896-x

Gupta, N., Gond, S. and Gupta, S.K. 2022. Spatiotemporal trend characteristics of rainfall and drought jeopardy over Bundelkhand Region, India. Arab. J. Geosci., 15(12): 1155. https://doi.org/10.1007/s12517-022-10389-8

Gupta, S.K., Gupta, N. and Singh, V.P. 2021. Variable-sized cluster analysis for 3d pattern characterization of trends in precipitation and change-point detection. J. Hydrol. Eng., 26(1): 04020056. https://doi.org/10.1061/(asce)he.1943-5584.0002010

He, X., Wada, Y., Wanders, N. and Sheffield, J. 2017. Intensification of hydrological drought in California by human water management. Geophys. Res. Lett., 44(4): 1777-1785. https://doi.org/10.1002/2016GL071665

Huang, C., Zhang, Q., Singh, V.P., Gu, X. and Shi, P. 2017. Spatio-temporal variation of dryness/wetness across the Pearl River basin, China, and relation to climate indices. Int. J. Climatol., 37: 318-332. https://doi.org/10.1002/joc.5005

Liu, X.F., Wang, S.X., Zhou, Y., Wang, F.T., Yang, G. and Liu, W.L. 2016. Spatial analysis of meteorological drought return periods in China using Copulas. Natural Hazards, 80(1): 367-388. https://doi.org/10.1007/s11069-015-1972-7

Malik, A., Kumar, A., Kisi, O., Khan, N., Salih, S. Q. and Yaseen, Z. M. 2021. Analysis of dry and wet climate characteristics at Uttarakhand (India) using effective drought index. Natural Hazards, 105(2), 1643-1662. https://doi.org/10.1007/s11069-020-04370-5

Mallya, G., Mishra, V., Niyogi, D., Tripathi, S. and Govindaraju, R. S. 2015. Trends and variability of droughts over the Indian monsoon region. Weather Clim. Extremes, 12: 43-68. https://doi.org/10.1016/j.wace.2016.01.002

Mesbahzadeh, T., Mirakbari, M., Mohseni Saravi, M., Soleimani Sardoo, F. and Miglietta, M.M. 2020. Meteorological drought analysis using copula theory and drought indicators under climate change scenarios (RCP). Meteorol. Appl. 27(1): 1-20. https://doi.org/10.1002/met.1856

Mishra, A.K. and Singh, V.P. 2010. A review of drought concepts. J. Hydrol., 391(1-2): 202-216. https://doi.org/10.1016/j.jhydrol.2010.07.012

Nabaei, S., Sharafati, A., Yaseen, Z.M. and Shahid, S. 2019. Copula

based assessment of meteorological drought characteristics: Regional investigation of Iran. Agric. Forest Meteorol., 276-277:, 107611. https://doi.org/10.1016/j.agrformet.2019.06.010

Omar, P.J., Dwivedi, S.B. and Dikshit, P.K. 2019a. Temporal variability study in rainfall and temperature over Varanasi and adjoining areas. Disas. Adv., 12(1): 1-7.

Omar, P.J., Gaur, S., Dwivedi, S.B. and Dikshit, P.K.S. 2019b. Groundwater modelling using an analytic element method and finite difference method: An insight into Lower Ganga river basin. J. Earth Syst. Sci., 128(7): 195. https://doi.org/10.1007/s12040-019-1225-3.

Omar, P.J., Gaur, S., Dwivedi, S.B. and Dikshit, P.K.S. 2020. A modular three-dimensional scenario-based numerical modelling of groundwater flow. Water Resour. Manag., 34(6): 1913-1932. https://doi.org/10.1007/s11269-020-02538-z

Pandey, V., Srivastava, P. K., Singh, S.K., Petropoulos, G.P. and Mall, R.K. 2021. Drought identification and trend analysis using long-term chirps satellite precipitation product in Bundelkhand, India. Sustainability (Switzerland), 13(3): 1-20. https://doi.org/10.3390/su13031042

Pei, Z., Fang, S., Wang, L. and Yang, W. 2020. Comparative analysis of drought indicated by the SPI and SPEI at various timescales in inner Mongolia, China. Water, 12(7): 925. https://doi.org/10.3390/w12071925

Polong, F., Chen, H., Sun, S. and Ongoma, V. 2019. Temporal and spatial evolution of the standard precipitation evapotranspiration index (SPEI) in the Tana River Basin, Kenya. Theor. Appl. Climatol., 138(1-2): 777-792. https://doi.org/10.1007/s00704-019-02858-0

Qutbudin, I., Shiru, M.S., Sharafati, A., Ahmed, K., Al-Ansari, N., Yaseen, Z.M., Shahid, S. and Wang, X. 2019. Seasonal drought pattern changes due to climate variability: Case study in Afghanistan. Water, 11(5): 096. https://doi.org/10.3390/w11051096

Singh, G. 2019. Rainfall analysis for crop planning under rainfed condition at Mirzapur district in Vindhya plateau of Indo-Gangetic Plain Rainfall analysis for crop planning under rainfed condition at Mirzapur district in Vindhya plateau of Indo-Gangetic Plain. Indian J. Soil Conserv., 47(1): 1-8.

Singh, G., Soil, C. and Singh, R.M. 2019. Stochastic modeling of water deficit for crop planning under climatic conditions of Mirzapur district in Uttar Pradesh Stochastic modeling of water deficit for crop planning under climatic conditions of Mirzapur district in Uttar Pradesh. J. Agrometeorol., 21: 41-47.

Srinivas, P. and Sarala, C. 2007. Hydrological data analysis for the identification of droughts in Anantapur District, Andhra Pradesh. Nature Environ. Pollut. Technol., 6(4): 565-572.

Subbiah, T.S., Parthiban, P., Mahesh, R. and Das, A. 2021. Time series analysis of decadal precipitation pattern at selected cities of southern India. Nature Environ. Pollut. Technol., 20(3): 1201-1208. https://doi.org/10.46488/NEPT.2021.v20i03.028

Rosalia, A.C. and Hakim, L. 2021. Spatial analysis of the impact of flood and drought on food security index. Nature Environ. Pollut. Technol., 20(2): 721-727. https://doi.org/10.46488/NEPT.2021.v20i02.031

Tan, C., Yang, J. and Li, M. 2015. Temporal-spatial variation of drought indicated by SPI and SPEI in Ningxia Hui autonomous region, China. Atmosphere, 6(10): 1399-1421. https://doi.org/10.3390/atmos6101399

Thornthwaite, C.W. 1948. An approach toward a rational classification of climate. Geogr. Rev., 38(1): 55. https://doi.org/10.2307/210739

Varughese, A. 2017. Analysis of historical climate change trends in Bharathapuzha River Basin, Kerala, India. Nature Environ. Pollut. Technol., 16(1): 237-242.

Vicente-Serrano, S.M., Beguería, S. and López-Moreno, J.I. 2010. A multiscalar drought index sensitive to global warming: The standardized precipitation evapotranspiration index. J. Clim., 23(7): 1696-1718. https://doi.org/10.1175/2009JCLI2909.1

Yevjevich, V. 1969. An objective approach to definitions and investigations of continental hydrologic droughts. J. Hydrol., 7(3): 353. https://doi.org/10.1016/0022-1694(69)90110-3

Zhang, D.D., Yan, D.H., Lu, F., Wang, Y.C. and Feng, J. 2015. Copula-based risk assessment of drought in Yunnan province, China. Natural Hazards, 75(3): 2199-2220. https://doi.org/10.1007/s11069-014-1419-6